EFFECT OF BEAM – COLUMN INTERACTION ON AXIAL COMPRESSIVE FORCE IN POST–TENSIONED CONTINUOUS CONCRETE BEAM

By

Kojo Amponsah Nkuako
B.S., Kwame Nkrumah University of Science and Technology, 2009

A Thesis
Submitted in Partial Fulfillment of the Requirements for the
Master of Science Degree.

Department of Civil Engineering
in the Graduate School
Southern Illinois University Carbondale
December 2013

THESIS APPROVAL

EEFECT OF BEAM – COLUMN INTERACTION ON AXIAL COMPRESSIVE FORCE IN POST–TENSIONED CONTINUOUS CONCRETE BEAM

By

Kojo Amponsah Nkuako

A Thesis Submitted in Partial

Fulfillment of the Requirements

for the Degree of

Master of Science

in the field of Civil Engineering

Approved by:

Dr. J. Kent Hsiao, Chair

Dr. Aslam Kassimali

Dr. Jale Tezcan

Graduate School
Southern Illinois University Carbondale
October 2013

AN ABSTRACT OF THE THESIS OF

KOJO AMPONSAH NKUAKO, for the Master of Science degree in Civil Engineering, presented on 3rd October 2013, at Southern Illinois University Carbondale.

TITLE: EFFECT OF BEAM – COLUMN INTERACTION ON AXIAL COMPRESSIVE FORCE IN POST–TENSIONED CONTINUOUS CONCRETE BEAM

MAJOR PROFESSOR: Dr. J. Kent Hsiao

This research seeks to investigate the instantaneous effect of beam – column interaction on the axial compressive force in post-tensioned continuous concrete beam. Hypothetically, if a prestressed beam is connected to columns, the axial compressive force in the concrete of the beam caused by the prestressed force will be reduced due to the interaction between the beam and the columns during post-tensioning.

Finite Element Approach usually has been considered the most accurate approach for structural analysis. However, Load Balancing Approach has commonly been used by structural engineers to analyze prestressed concrete structures. Load Balancing Approach converts the post-tensioned force to uniform distributed loads to be applied to models of concrete frames.

The scope of work in this research involved making out two concrete frames as research subjects, developing frame models for SAP2000 prestressing approach and the Load Balancing Method. Static linear analysis was performed on both approaches to verify the hypothesis mentioned above.

ACKNOWLEDGEMENTS

I would like to thank my family for their boundless love and support in my pursuit of goals and aspirations.

I would like to express great depths of gratitude to Professor Kent Hsiao for his valuable guidance and suggestions during the course of my work, which provided a great first-hand experience with the research community and led to the successful completion of this thesis. To the Civil and Environmental Engineering Department, I would say thank you for the inspiration and opportunities afforded me, it's really been an exciting journey. I wish to thank my colleagues and friends who have helped me during my time in Southern Illinois University Carbondale graduate school. Finally, I would say trust in God.

TABLE OF CONTENTS

LIST OF TABLES

TABLE PAGE

LIST OF FIGURES

CHAPTER 1

INTRODUCTION

A major 21st century alternative in concrete construction schemes is the usage of the concept of prestressing. Most notable of such construction evolution is the employment of post-tensioning technique in reinforced concrete structural systems. This affords engineers the ability to achieve feats such as meeting the aesthetic appeal of their clientele, highly competitive initial cost saving compared to construction by other methods, low maintenance cost and the obvious speed of construction (Feyermuth, 2005).

Coupled with post-tensioning, is the utilization of continuous beams in the design of reinforced concrete and other structural systems. Continuity affords the designers desirable features like lowering the stresses and moments at midspans. This results in concrete beams that are shallower and stiffer as compared to simply supported beams. Therefore, reduced cost of materials and construction result from the merit of designing lighter structures with lighter foundations.

However, these advantages do not come without set-backs. Post-tensioned concrete beams connected to columns may cause a reduction in the axial compressive forces in the concrete of the beam. It is commonplace to ignore losses due to restraints in the analysis of the post-tensioned concrete beams. American Concrete Institute (ACI-318) proposes that losses due to restraining effects, which could be fairly significant, should be accounted for in designs in order for structural systems to possess the desired behavior. The development of lateral forces and moments in the supporting columns also warrants additional reinforcements at these

supports. Lastly, continuity in post-tensioned concrete beams does come with the disadvantage of developing degrees of frictional losses depending on the complexity of the tendon profile.

Research and experience have continuously contributed to safe and economical ways of addressing these concerns. Moreover, through appropriate design and construction of the final structural system, these set-backs could be fairly alleviated.

1.1 Research Goals

The goals of this research are to:

1. Determine the axial compressive forces in the post-tensioned continuous concrete beams of two two – bay, one – storey concrete frames at the time of initial prestress transfer.
2. Determine the adequacy of Load Balancing Method in estimating the net axial compressive forces in the post-tensioned continuous concrete beams of both frames at the time of initial prestress transfer.
3. Compute the extreme concrete fiber stresses of the post-tensioned continuous concrete beams of both frames at the time of initial prestress transfer.

CHAPTER 2

LITERATURE REVIEW

2.1 Effects Due to Restraints

For simply supported beam, the effect of prestressing is the axial force equal to the prestressing force. However, a concrete beam rigidly restrained by adjoining columns leads to compressive force deficits in the concrete of the beam.

If a concrete beam is not allowed to deform freely under compressive force, part of the compressive force is lost to the adjoining columns. The reactions generated at the support location of the adjoining columns are evidence of these deficits. Subsequent temperature differentials also leads to further transfer of the force to the restraining columns (Kelley, 2000).

2.2 Tendon Discretization Method

Tendon Discretization is one of three modeling techniques that models the effect of the tendon as a loading component of the hosting element resisting any external applied loading (Alami, 2000). The other two techniques are load balancing and modeling through primary moments.

Tendon Discretization technique offers a more accurate estimation of the effect of immediate prestressing force application on the concrete beam taking into account the level of complexity of the tendon profile. It utilizes an iterative procedure in which the immediate

prestress losses are computed based on the current prestressing force. The procedure is continued until convergence is reached. Hence, wobble and curvature friction losses arising from the bends in parabolic tendon profiles and seating losses at jacking ends are incorporated in the analysis results.

With this technique, the parabolic tendon profile is transformed into a continuous series of straight sloping segments. The force in each segment is transformed into equivalent horizontal and vertical component forces. The component forces are then transferred to the fibers of the hosting element in addition to a moment equal to the horizontal component times the eccentricity from the centroid of the hosting element. It is with this technique that SAP2000 prestressing approach was based on.

2.3 Load Balancing Method

Load Balancing Method (LBM) is a technique based on utilizing the vertical force of the draped or harped prestressing tendon to counteract or balance the imposed loading, either uniformly distributed loads or point loads, to which a concrete structural member is subjected to.

Load Balancing Method introduced by T. Y. Lin (Lin, 1963) is one of the three methods of prestressed concrete design and analysis. The other two techniques are the stress – concept which analyses prestressed concrete with respect to its elastic stresses and the strength – concept which deals with its ultimate strength.

LBM offers the simplest approach to prestressed concrete design and analysis. For statically determinate structures, the advantage of the LBM is not significant. However, when

dealing with statically indeterminate structures, LBM offers tremendous advantages over the other two methods in terms of visualization and calculations.

The concept behind load balancing is illustrated in the simply supported beam diagram shown.

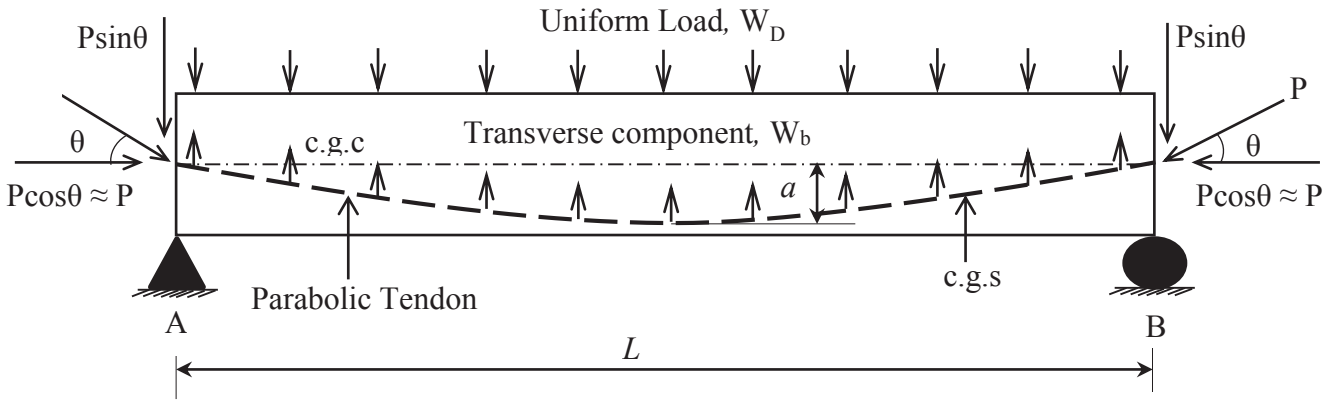

Fig. 2-1 Balancing of a Uniform Imposed Load

Where,

W_D = Imposed gravity loading, kip/in.

W_b = Balancing uniformly distributed load, kip/in.

P = Prestressing force, kip

L = Length of parabolic section, in.

a = Tendon's drape, in.

θ = Jacking angle, degrees

c.g.c. = Center of gravity of the concrete

c.g.s. = Prestressing tendon profile

Given the prestressing force (P), length of the parabolic section (L) and tendon's drape (a), the balancing uniformly distributed load (W_b) is computed by Equation 1 (Lin, 1963).

$$W_b = {}^{8Pa}/_{L^2} \quad (1)$$

After load balancing, the analysis of prestressed simply supported beam is reduced to a non-prestressed beam as illustrated in Figure 2-2.

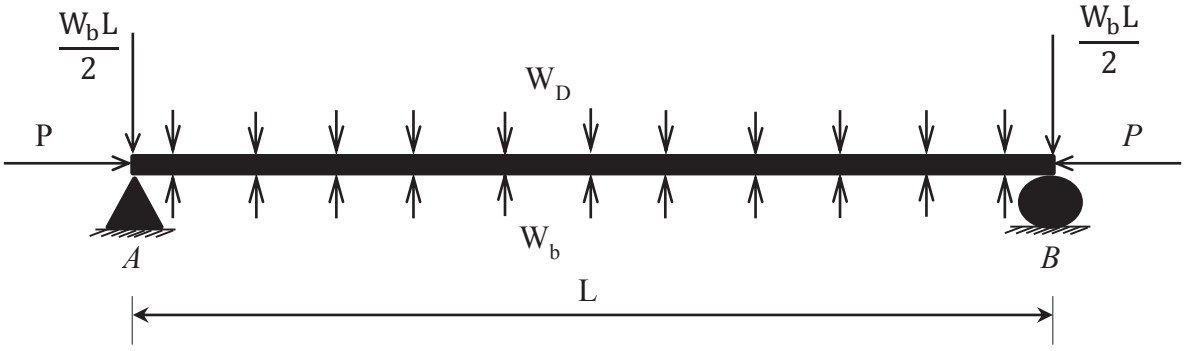

Fig. 2-2 Simply Supported Non-prestressed Beam

Research conducted have shown that neglecting the axial prestressing force during frame analysis has a substantial effect on the resultant axial forces and moments induced in the concrete columns (Mohammed, 2012). Further deformation and axial force are introduced to the

supporting columns. Therefore, it is of prime importance to apply the horizontal (axial) component of the prestressing force in the analysis of prestressed concrete frame structures.

If the external applied load, including the dead load of the concrete beam, is exactly balanced by the transverse component of the prestressing force, there is no bending in the beam. Hence, the beam is considered to be under a uniform compressive force (F).

Given the axial compressive force (F) which is equal to the prestressing force (P) and cross-sectional area (Ac), the concrete fiber stresses due to the axial compressive force (f) is computed by Equation 2.

$$f = {}^{P}/_{A_c} \qquad (2)$$

However, if the external load is not completely balanced by the prestressing force, bending or flexural stresses results.

Referring to Figure 2-2, the unbalanced bending moment due to prestressing force (M_{ub}) is computed by Equation 3.

$$M_{ub} = M_D - M_b \qquad (3)$$

Where,

M_D = Moment due to the self-weight of the beam, kip-in. (positive moment)

M_b = Balancing moment provided by the prestressing force, kip-in. (negative moment)

Hence, the bending stress (f) due to the unbalanced bending moment (Mub) is computed by Equation 4.

$$f = {}^{M_{ub}y}/_{I} \quad (4)$$

Where,

y = Distance to top or bottom of the cross-section from the center of gravity, in.

I = Moment of inertia of the cross-section of the beam, in^4.

Therefore, the effective stress is computed by Equation 5 with the negative sign indicating stresses in compression and the positive sign indicating stresses in tension.

$$f = -{}^{P}/_{A_c} \pm {}^{M_{ubi}}/_{S} \quad (5)$$

Where, S = Sectional modulus of the concrete section, in^3.

$$S = {}^{I}/_{y} \quad (6)$$

2.4 ACI – 318 Flexural Requirements

ACI-318 makes the following serviceability requirements for flexural members at time of initial prestress transfer:

1. Extreme concrete fiber stresses in compression shall not exceed $0.6f'_{ci}$
2. Extreme concrete fiber stresses in tension shall not exceed $3\sqrt{f'_{ci}}$

Where,

f'_{ci}, = Specified compressive strength of concrete at time of initial prestressing, psi

The initial compressive stress, f'_{ci}, of concrete can be computed with Equation 7 (Nawy, 2009).

$$f'_{ci} = \left(t/4 + 0.85t\right) f_c \quad (7)$$

Where,

f_c = Specified compressive strength of concrete at 28 days, psi

t = Time of post-tensioning, days, which is commonly 7 days

CHAPTER 3

METHODOLOGY

Step-by-step approach for the modeling of the post-tensioned continuous concrete frames using SAP2000 prestressing approach and Load Balancing Method are presented as follows.

3.1 Boundary Conditions

The excitation forces for the Load Balancing Method (LBM) was the prestressing force at anchorage (initial prestressing force). Therefore, friction, elastic shortening and anchorage slip were inherently accounted for in the estimation of the prestressing force.

However, the initial prestressing force computed for the LBM was used as the jacking force for the SAP2000 prestressing approach. This aided in ascertaining whether the change in stress along the tendon length could have a significant effect in the analysis results of the Load Balancing Method. Long – term prestress losses including creep stress, shrinkage stress and steel relaxation were not considered when modeling the tendons.

The continuous concrete beams of the frames were prismatic with no change to their centroidal axis. The three supporting columns were also prismatic having constant material and geometric properties.

Monolithic beam-column connections were assumed for both models and hence, were modeled as such. The support conditions at the base of the columns were modeled fixed.

3.2 Models

Two documented numerical examples were found and researched on. These examples consisted of a prismatic concrete continuous beam over three concrete supporting columns.

The first design example (Hurst, 1998) with some modification to the support conditions will henceforth be referred to as Model 1.

Figures 3-1 and 3-2 show the tendon layout, and geometric and sectional properties respectively for Model 1.

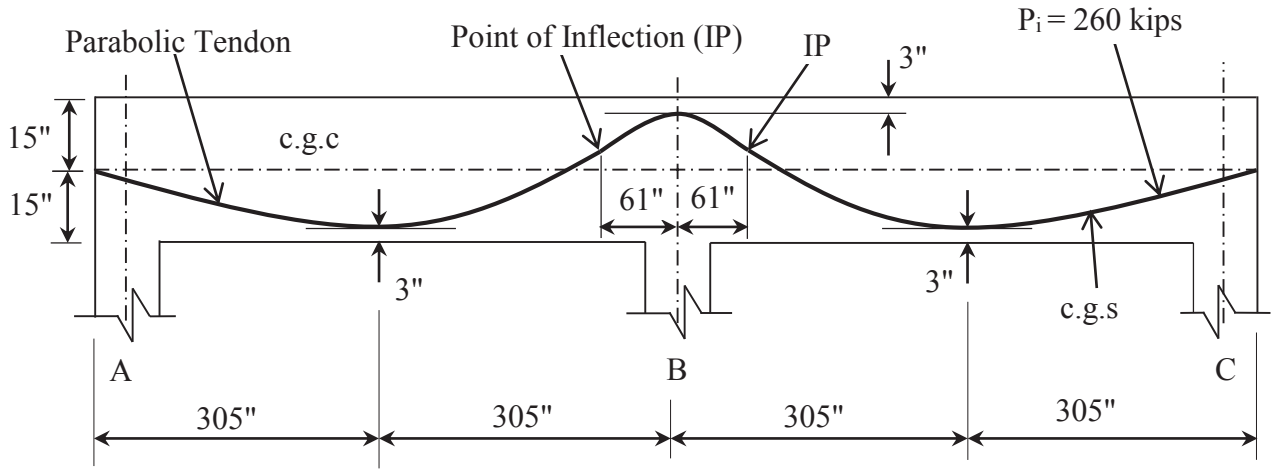

Fig. 3-1 Tendon Layout of Model 1

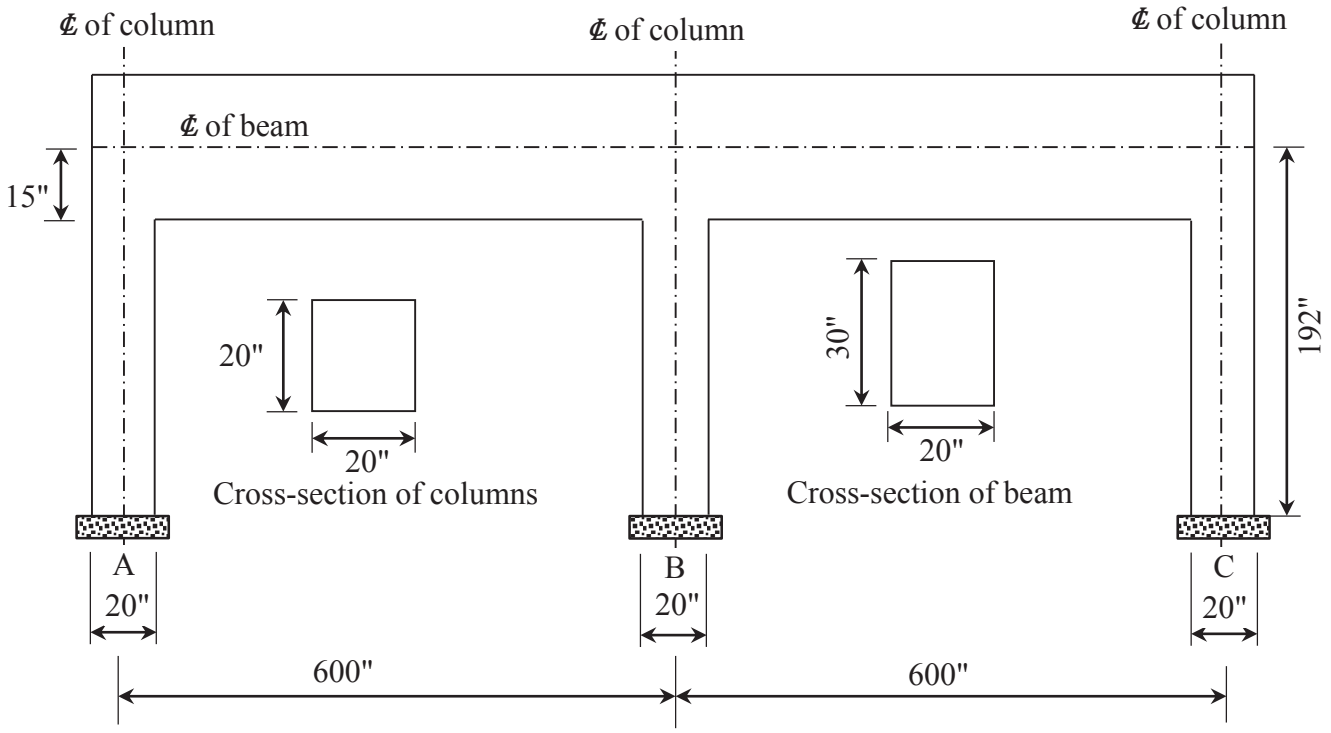

Fig. 3-2 Geometric and Sectional Properties of Model 1

The point of inflection (IP) is typically 10% of the respective spans. Hence, considering the left span of the continuous concrete beam of Model 1:

$IP = 0.1L = 0.1 \times 610" = 61"$

The second design example (Alami, 2000) with some modification to the support conditions will henceforth be referred to as Model 2.

Figures 3-3 and 3-4 show the tendon layout, and geometric and sectional properties respectively for Model 2.

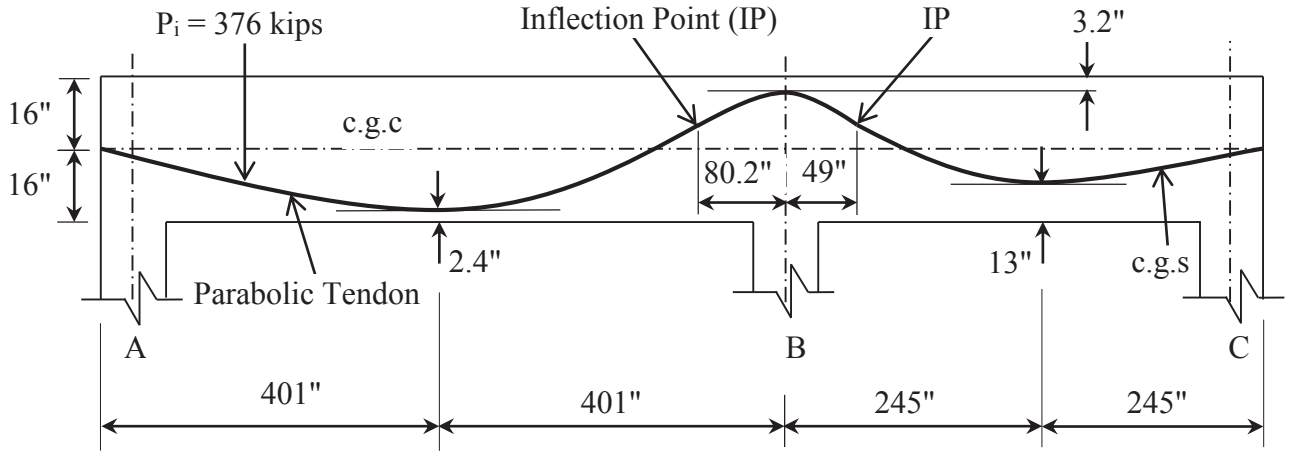

Fig. 3-3 Tendon Layout of Model 2

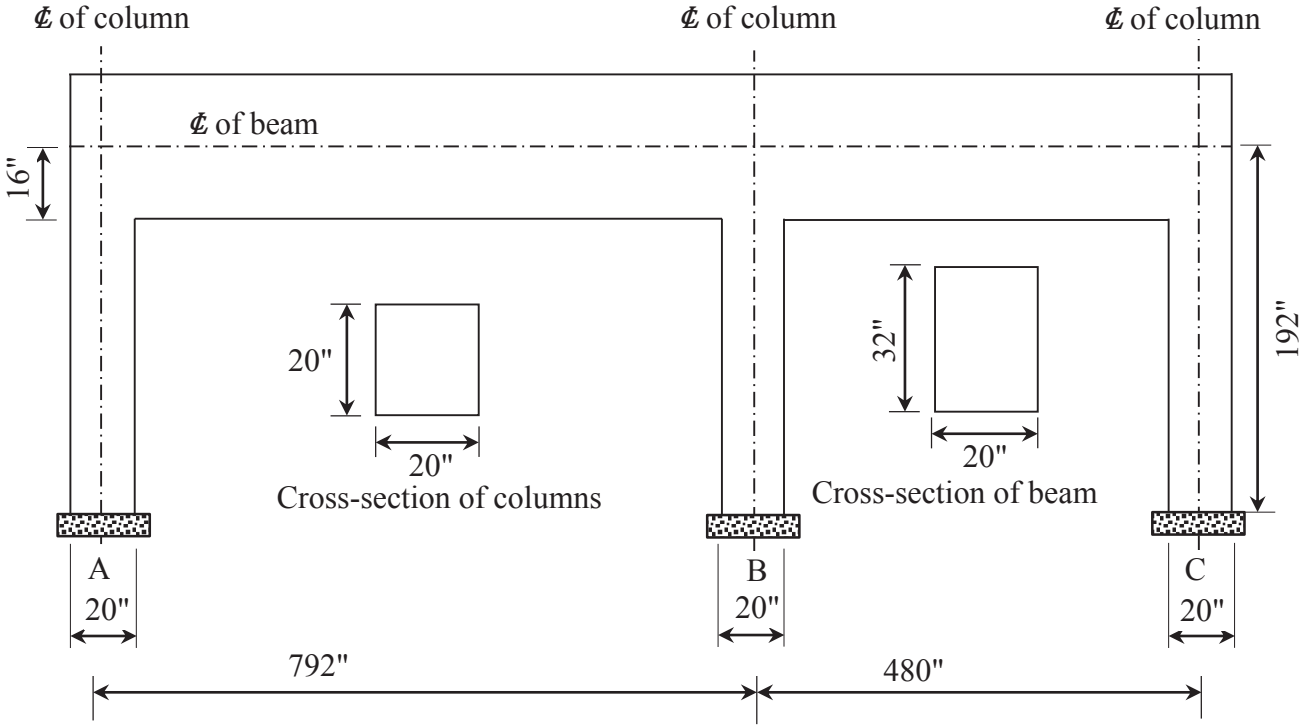

Fig. 3-4 Geometric and Sectional Properties of Model 2

The clear column heights for Model 1 and Model 2 were 177" and 176" respectively. Detailed sectional properties of both continuous beams for Models 1 and 2 are tabulated in the appendix.

The specified tensile strength, (f_{pu}), of the low-relaxation seven – wire strand used for both models was 270,000 psi (ASTM A416Gr270). The initial prestressing forces were computed according to ACI-318 standards.

For Model 1, a 9 - $^{1}/_{2}$" -dia-seven-wire-strand was used.

Hence, area of prestressing steel $(A_{ps}) = 9 \times 0.153 = 1.377$ in^2.

Initial prestress before losses $(f_{pi}) \cong 0.7 \times f_{pu} = 0.7 \times 270{,}000$

$= 189{,}000$ psi

Initial prestressing force before losses $(P_i) = A_{ps} \times f_{pi} = 1.377 \times 189{,}000$

$= 260{,}253$ Ib ≈ 260 kips

For Model 2, a 13- $^{1}/_{2}$" - dia-seven-wire-strand was used.

Hence, area of prestressing steel $(A_{ps}) = 13 \times 0.153 = 1.989$ in^2.

Initial prestress before losses $(f_{pi}) \cong 0.7 \times f_{pu} = 0.7 \times 270{,}000$

$= 189{,}000$ psi

Initial prestressing force before losses $(P_i) = A_{ps} \times f_{pi} = 1.989 \times 189{,}000$

$= 375{,}921$ Ib ≈ 376 kips

The elastic modulus (E_c) for high – strength concrete for the post-tensioned concrete beams and columns for both models was computed by Equation 8.

$$E_c = (40{,}000\sqrt{f'_c} + 10^6) \times \left(W_c/145\right)^{1.5} \quad \text{(Nawy, 2009).} \qquad (8)$$

Where,

W_c = Unit weight of concrete only = 145 Ib/ft^3

f'_c = Specified compressive strength at 28 days = 6,000 psi (Alami, 2000).

The elastic modulus for the high – strength concrete, E_c=4,098,387 psi.

The Poisson's ratio of the concrete used for both models was 0.2 (Nawy, 2009).

3.3 SAP2000 Prestressing Approach

The tendon was specified as a type of line object connected to the exterior joints of the two span continuous concrete beams. The tendons were modeled as loads acting internally in the beams.

The tendons were jacked simultaneously at both ends of the continuous concrete beams with jacking forces equal to the initial prestressing forces computed in sub-chapter 3.2.

Figures 3-5 and 3-6 show Model 1A and Model 2A respectively under the application of jacking force only using SAP2000 prestressing approach.

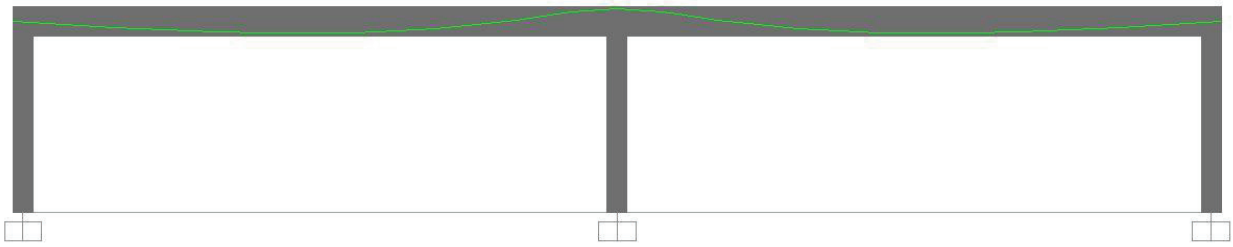

Fig. 3-5 Model 1A

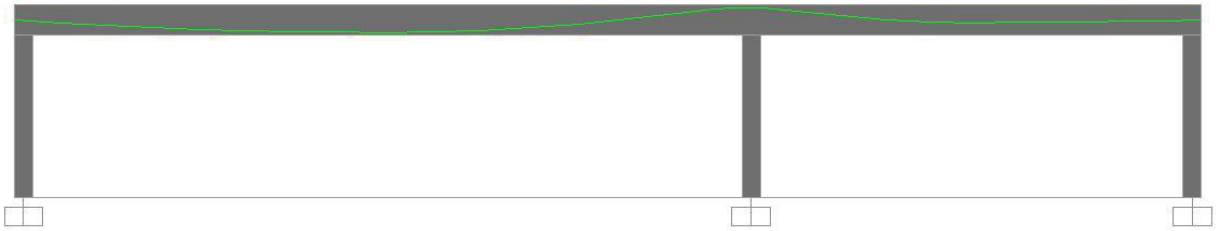

Fig. 3-6 Model 2A

3.4 Load Balancing Approach

Model 1B and Model 2B were modeled and assigned the same geometric, sectional and material properties as Model 1A and Model 2A respectively. The applied loads for these models were the balancing loads due to initial prestressing force and the horizontal (axial) component of the initial prestressing force. The balancing loads included vertical uniformly distributed loads acting along the length of the continuous concrete beams and vertical component of the initial

prestressing force acting perpendicularly to the center of gravity of the continuous concrete beams at the jacking points.

Figures 3-7 and 3-8 illustrate the geometric properties of the tendon layout of Model 1B for the computations of the balancing forces for the Load Balancing Method.

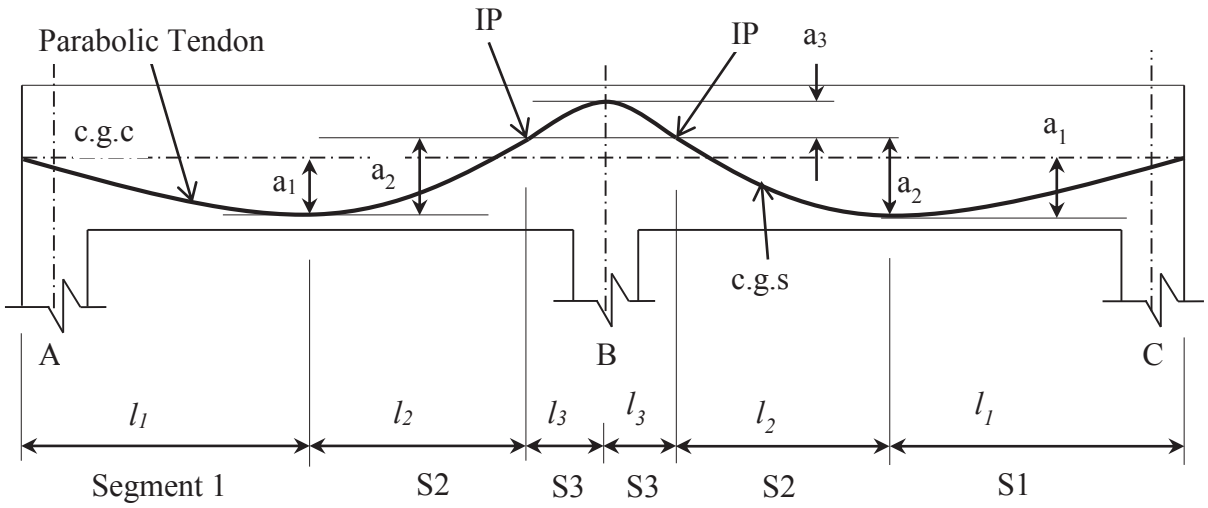

Fig. 3-7 Tendon Layout and Drapes of Model 1B

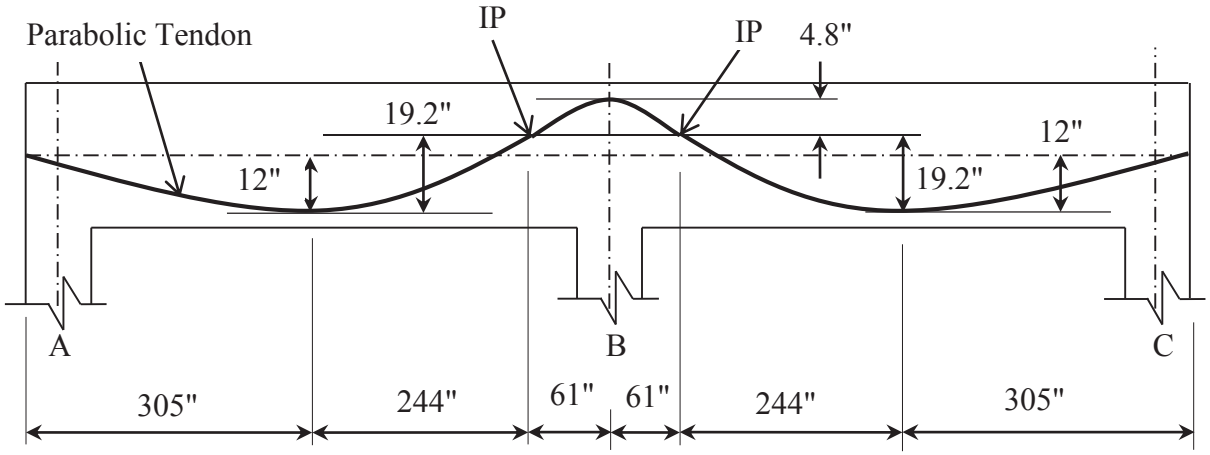

Fig. 3-8 Segment Lengths and Tendon's Drapes of Model 1B

Figures 3-9 and 3-10 illustrate the geometric properties of the tendon layout of Model 2B for the computations of the balancing forces for the Load Balancing Method.

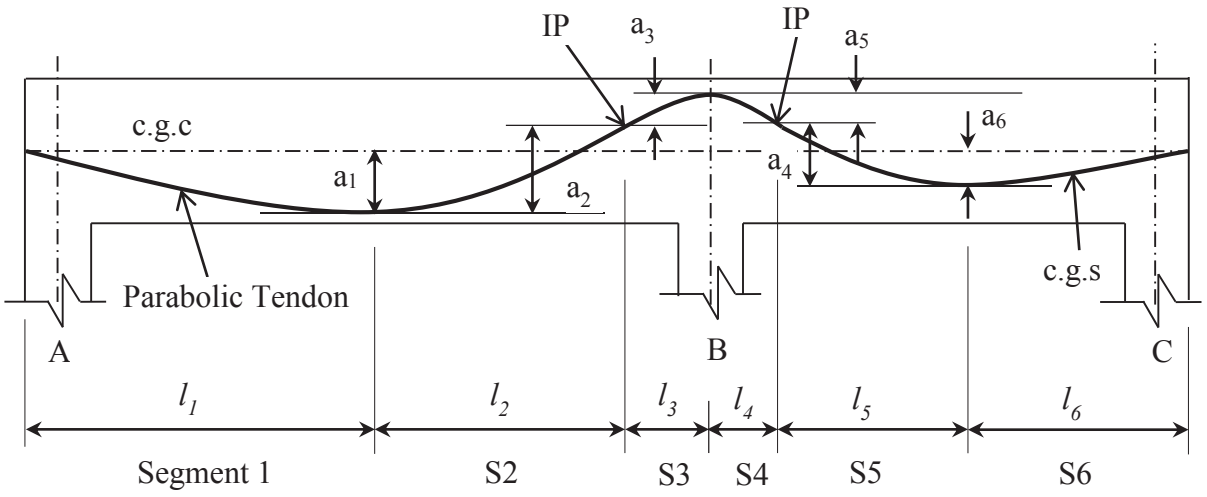

Fig. 3-9 Tendon Layout and Drapes of Model 2B

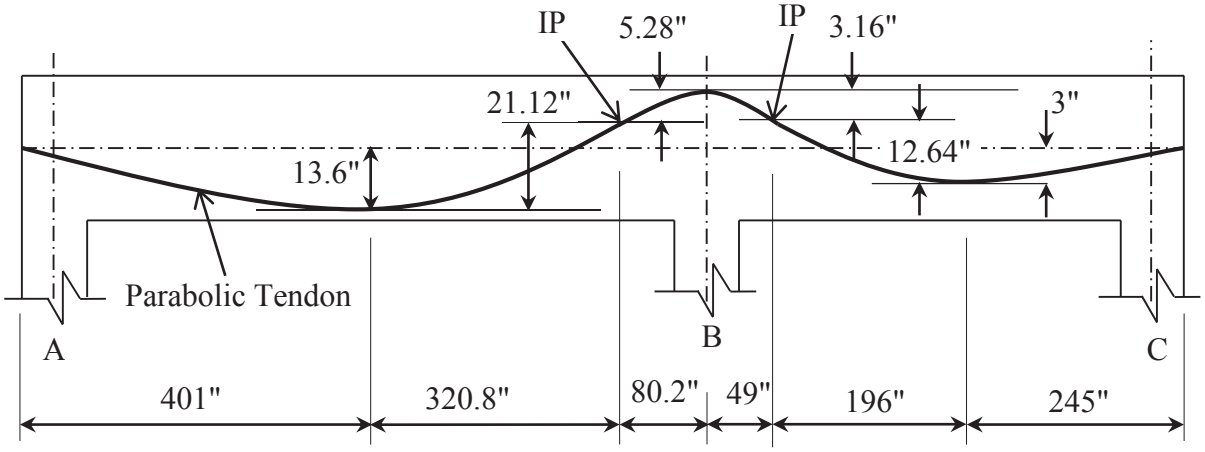

Fig. 3-10 Segment lengths and Tendon's Drapes of Model 2B

Given the initial prestressing force (P_i), tendon's drape (a), parabolic section length (L) for each segment, the balancing uniformly distributed load due initial prestressing force (W_{bi}) is given by Equation 1.

Therefore, the balancing uniformly distributed load for segment 1 of Model 1B was computed as follows:

$$W_{bi1} = \frac{8 \times 260 \times 12}{610^2} = 0.0671 \text{ kip/in. } (\uparrow)$$

The vertical component of the initial prestressing forces (Piv) were applied at the jacking ends of the parabolic tendon to balance out the uniformly distributed loads due to initial prestressing force relating to ends A and C.

The vertical component of the initial prestressing force (Piv) of Model 1B were computed as follows:

P_{iv} @ end A = $W_{bi1} \times l_1 = 0.0671 \times 305 = 20.47$ kips ($\downarrow$)

P_{iv} @ end C = $W_{bi6} \times l_6 = 0.0671 \times 305 = 20.47$ kips ($\downarrow$)

Similarly, the balancing uniformly distributed load for segment 1 of Model 2B was computed as follows:

$$W_{bi1} = \frac{8 \times 376 \times 13.6}{802^2} = 0.0636 \text{ kip/in. } (\uparrow)$$

The vertical component of the initial prestressing force (Piv) for Model 2B were also computed as follows:

P_{iv} @ end A = $W_{bi1} \times l_1 = 0.0636 \times 401 = 25.50$ kips ($\downarrow$)

P_{iv} @ end C = $W_{bi6} \times l_6 = 0.0376 \times 245 = 9.21$kips (↓)

Table 3-1 shows the parabolic section length (L), tendon's drape (a), initial prestressing force (Pi) and the corresponding balancing uniformly distributed loads (Wbi) for Model 1B.

Table 3-1 Balancing Loads for Model 1B

Segment	Segment Length (l), in.	Parabolic Section Length, L, in.	a, in.	P_i, kips	W_{bi}, kip/in.
1	305	610	12	260	0.0671 (↑)
2	244	488	19.2	260	0.1677 (↑)
3	61	122	4.8	260	0.6708 (↓)

The rest of the balancing uniformly distributed loads, i.e. W_{bi2} and W_{bi3}, cancel out for Model 1B:

$W_{bi2} \times l_2 = 0.1677 \times 244 = W_{bi3} \times l_3 = 0.6708 \times 61 = 40.92$ kips

Table 3-2 shows the parabolic section length (L), tendon's drape (a), initial prestressing force (P_i) and the corresponding balancing uniformly distributed loads (W_{bi}) for Model 2B.

Table 3-2 Balancing Loads for Model 2B

Segment	Segment Length (l), in.	Parabolic Section Length, L, in.	a, in.	P_i, kips	W_{bi}, kip/in.
1	401	802	13.6	376	0.0636 (↑)
2	320.8	641.6	21.12	376	0.1543 (↑)
3	80.2	160.4	5.28	376	0.6173 (↓)
4	49	98	3.16	376	0.9897 (↓)
5	196	392	12.64	376	0.2474 (↑)
6	245	490	3	376	0.0376 (↑)

The rest of the balancing uniformly distributed loads, i.e. W_{bi2} and W_{bi5} cancel out W_{bi3} and W_{bi4} respectively for Model 2B:

$W_{bi2} \times l_2 = 0.1543 \times 320.8 = W_{bi3} \times l_3 = 0.6173 \times 80.2 \approx 49.50$ kips

$W_{bi5} \times l_5 = 0.2474 \times 196 = W_{bi4} \times l_4 = 0.9897 \times 49 \approx 48.49$ kips

Figure 3-11 and Figure 3-12 illustrate both Model 1B and Model 2B respectively under balancing uniformly distributed loads (kip/in), and vertical and axial (horizontal) components (kips) of the initial prestressing force using SAP2000.

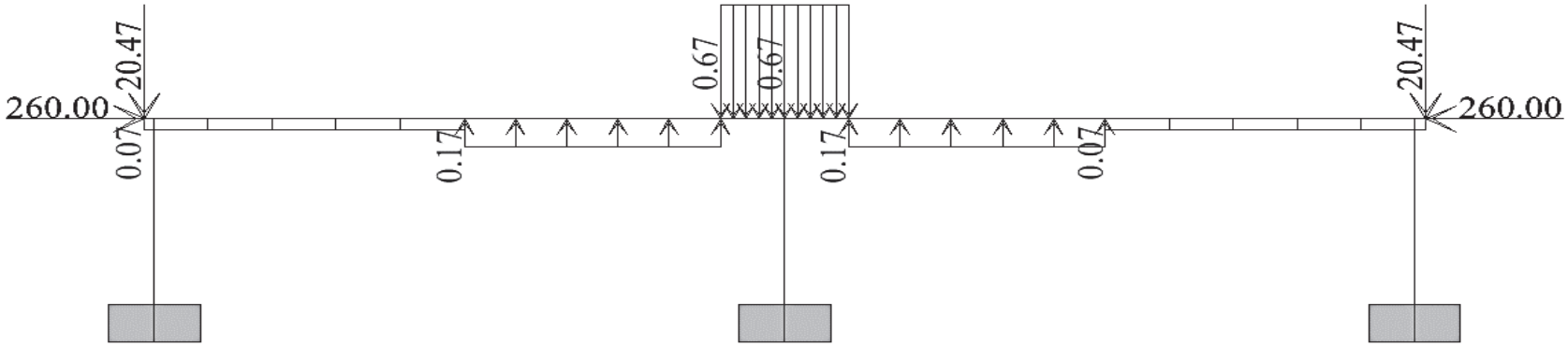

Fig. 3-11 Model 1B

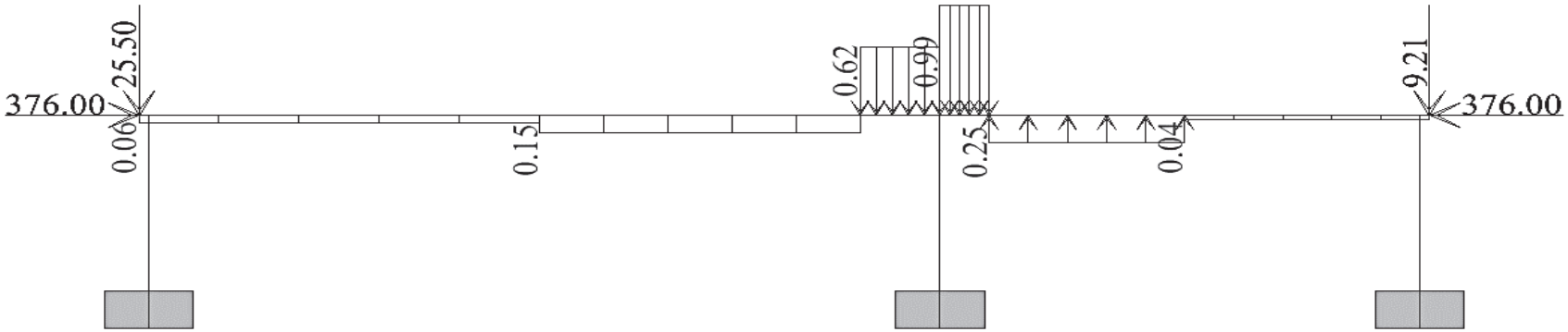

Fig. 3-12 Model 2B

Moreover, imposed dead load due to the self-weight of the beams (W_D) were computed for Models 1 and 2. Models 1C and 2C were created and assigned the same geometric, sectional and material properties as Model 1A and Model 2A.

Models 1C and 2C were under the action of horizontal (axial) and vertical component of the initial prestressing force, and the unbalanced uniformly distributed load due to initial prestressing force. These models were created for the computations of the extreme concrete fiber stresses at the time of initial prestress transfer.

Given the unit weight of concrete to be 150 Ib/ft^3, the self-weight of the continuous concrete beam for Model 1C was computed as follows:

$$W_D = \frac{600 \times 150}{1000 \times 1728} = 0.0521 \text{ kip/in. } (\downarrow)$$

Hence, the unbalanced uniformly distributed load due to initial prestressing force (W_{ubi}) for segment 1 of Model 1C was computed as follows:

$$W_{ubi} = W_D(\downarrow) + W_{bi}(\uparrow)$$

$$W_{ubi} = 0.0521(\downarrow) + 0.0671(\uparrow) = 0.0150 \text{ kip/in. } (\uparrow)$$

Table 3-3 show the imposed dead load (W_D), balancing uniformly distributed loads (W_{bi}) and the unbalanced uniformly distributed loads due to initial prestressing force (W_{ubi}) for each segment of Model 1C.

Table 3-3 Unbalanced Loads of Model 1C.

Segment	Imposed Dead Load (W_D), kip/in.	Balancing Load (W_{bi}), kip/in.	Unbalanced Load (W_{ubi}), kip/in.
1	0.0521 (↓)	0.0671 (↑)	0.0150 (↑)
2	0.0521 (↓)	0.1677 (↑)	0.1156 (↑)
3	0.0521 (↓)	0.6708 (↓)	0.7229 (↓)

Similarly, the self-weight for the continuous beam for Model 2C was computed as follows:

$$W_D = \frac{640 \times 150}{1000 \times 1728} = 0.0556 \text{ kip/in. } (\downarrow)$$

The unbalanced uniformly distributed load due to initial prestressing force (Wubi) for segment 1 of Model 2C was computed as follows:

$$W_{ubi} = W_D(\downarrow) + W_{bi}(\uparrow)$$

$$W_{ubi} = 0.0556(\downarrow) + 0.0636(\uparrow) = 0.0080 \text{ kip/in. } (\uparrow)$$

Table 3-4 shows the imposed dead load (W_D), balancing uniformly distributed loads (W_{bi}) and the unbalanced uniformly distributed loads due to initial prestressing force (W_{ubi}) for each segment of Model 2C.

Table 3-4 Unbalanced Loads of Model 2C.

Segment	Imposed Dead Load (W_D), kip/in.	Balancing Load (W_{bi}), kip/in.	Unbalanced Load (W_{ubi}), kip/in.
1	0.0556 (↓)	0.0636 (↑)	0.0080 (↑)
2	0.0556 (↓)	0.1543 (↑)	0.0988 (↑)
3	0.0556 (↓)	0.6173 (↓)	0.6729 (↓)
4	0.0556 (↓)	0.9897 (↓)	1.0453 (↓)
5	0.0556 (↓)	0.2474 (↑)	0.1919 (↑)
6	0.0556 (↓)	0.0376 (↑)	0.0180 (↓)

Figure 3-13 and Figure 3-14 illustrate both Model 1C and Model 2C under horizontal (axial) and vertical component of the initial prestressing force (kips), and unbalanced uniformly distributed loads (kip/in.) due to initial prestressing force using SAP2000.

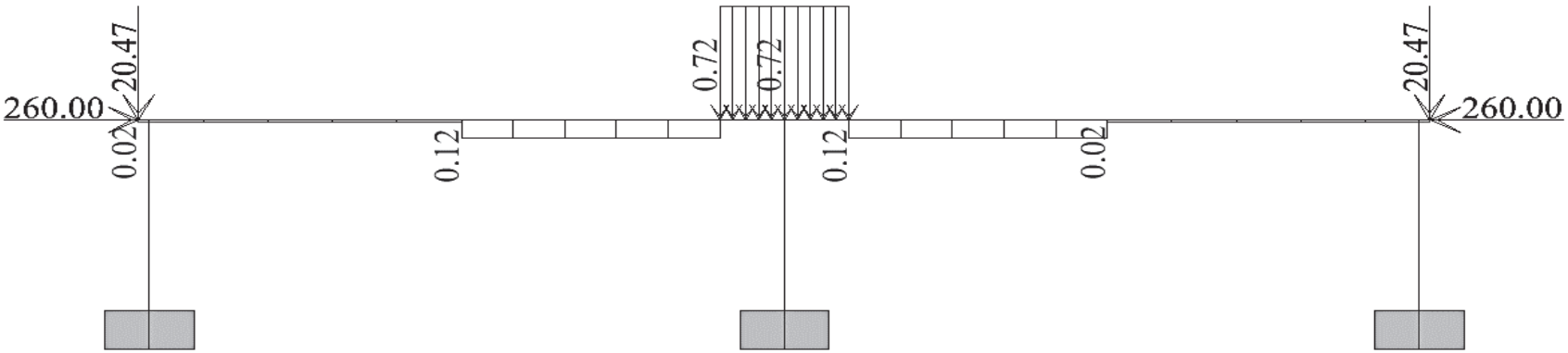

Fig.3-13 Model 1C

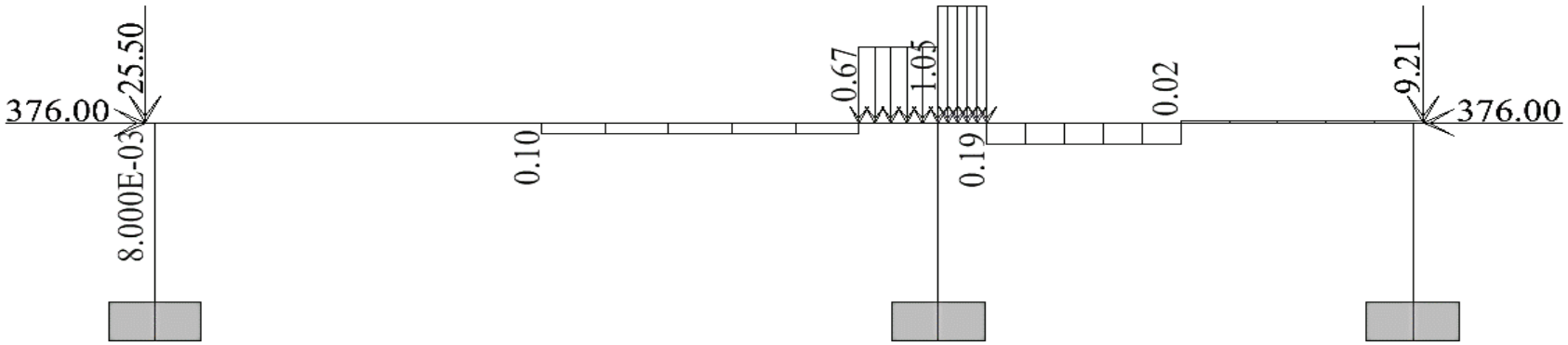

Fig. 3-14 Model 2C

CHAPTER 4

RESULTS

The support reactions, axial compressive forces and their corresponding absolute discrepancies at the time of initial prestress transfer from both SAP2000 prestressing approach and Load Balancing Approach are presented for both models. The extreme concrete fiber stresses at the time of initial prestress transfer were also computed using Load Balancing Approach for both models. Both approaches were subjected to static linear analysis in order to achieve the goals of this research.

Figures 4-1 and 4-2 show the deformed shapes for Model 1A and Model 2A respectively under balancing prestress loads after SAP2000 static linear analysis.

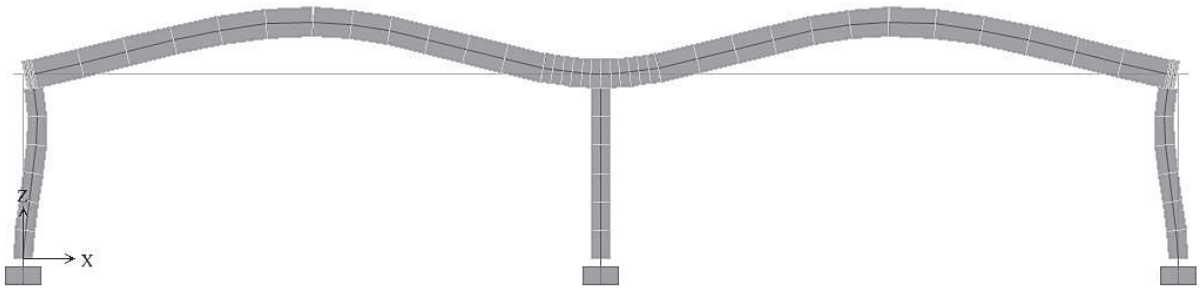

Fig. 4-1 Deformed Shape under Balancing Load of Model 1A

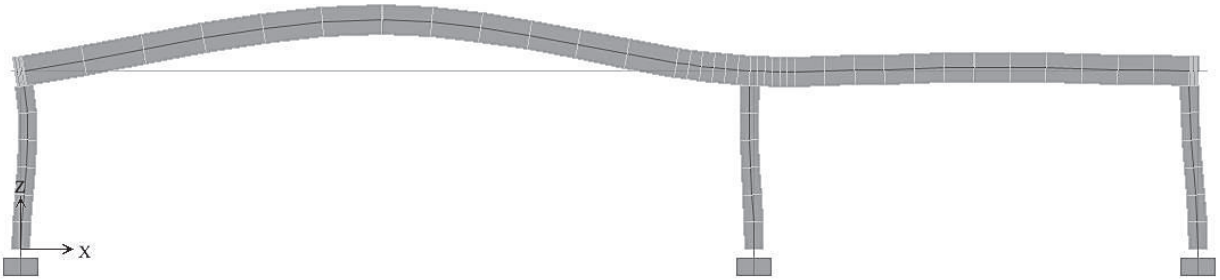

Fig. 4-2 Deformed Shape under Balancing Load of Model 2A

Figure 4-3 and Figure 4-4 show the support reactions of Models 1A and 1B.

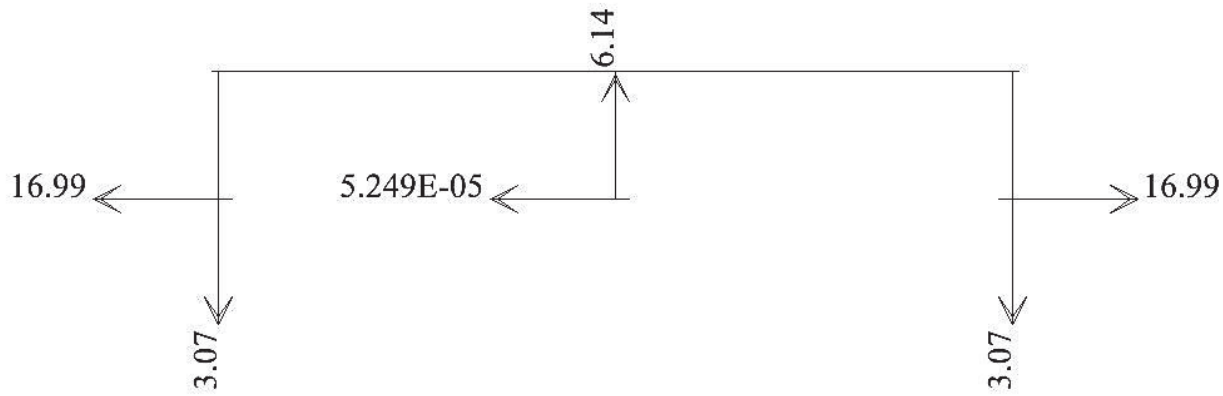

Fig. 4-3 Support Reactions (kips) of Model 1A

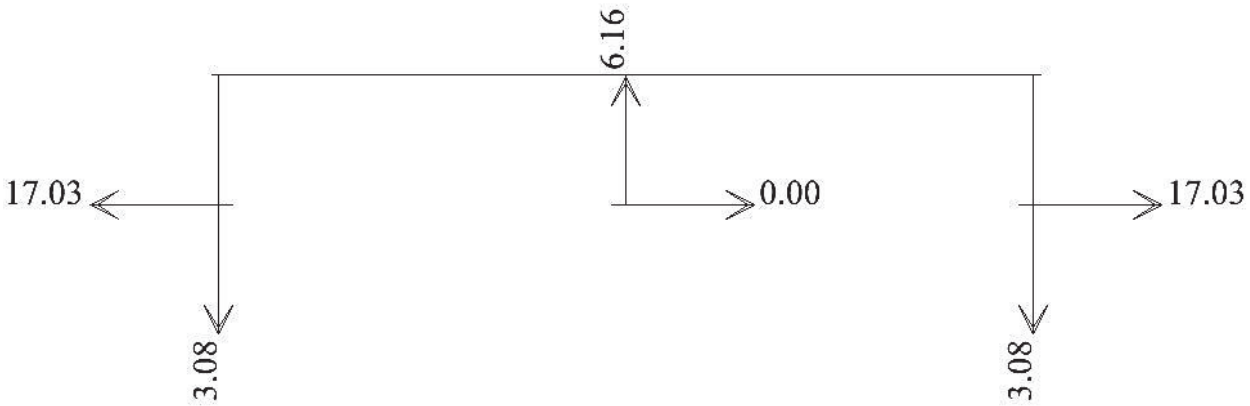

Fig. 4-4 Support Reactions (kips) of Model 1B

Model 1A maintained an average axial compressive force of 243.55 kips representing 6.33% deficit along the post-tensioned continuous concrete beam between the centerlines of the exterior columns A and C.

Figure 4-5 is the graphical representation of the axial compressive force distribution along the post-tensioned continuous concrete beam of Model 1A.

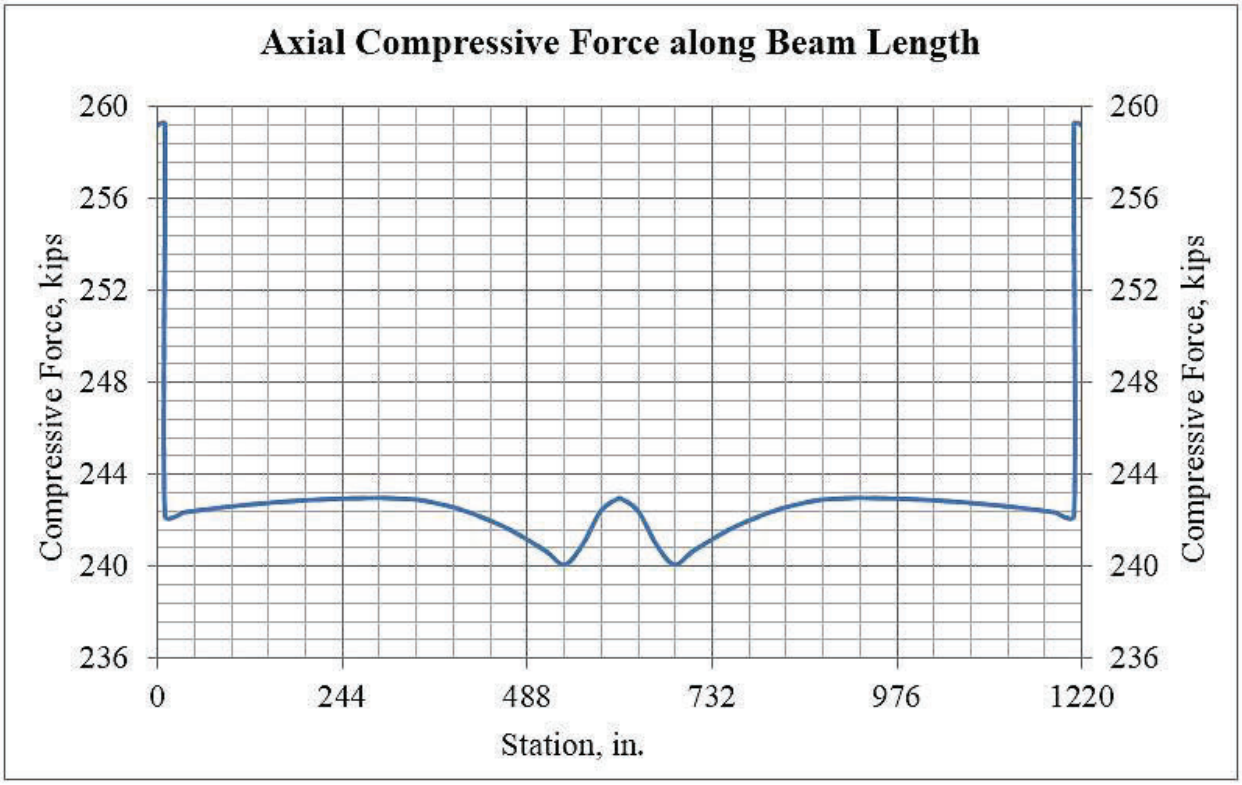

Fig. 4-5 Concrete Beam Compressive Force Distribution for Model 1A

Figure 4-6 shows the stations of interest along the post-tensioned continuous concrete beam, where the SAP2000 results of the axial compressive forces of both approaches were taken and tabulated for Model 1.

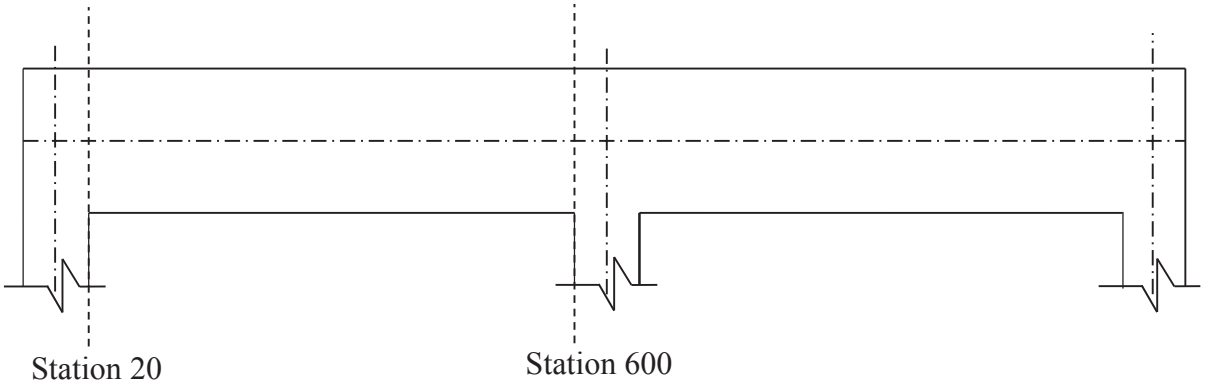

Fig. 4-6 Model 1 Result Stations

Table 4-1 shows the axial compressive forces, absolute discrepancies and their percentage discrepancies at the stations of interest along the post-tensioned continuous concrete beams of Model 1A and Model 1B.

Table 4-1 Axial Compressive Forces along Continuous Beams of Model 1A and Model 1B.

Station, in.	Axial Compressive Force (F), kips		Discrepancy, kips	Discrepancy%
Stations of Interest				
20	Model 1A	-242.300	0.672	0.277
	Model 1B	-242.972		
600	Model 1A	-242.778	0.194	0.080
	Model 1B	-242.972		

Figure 4-7 and Figure 4-8 show support reactions of Models 2A and 2B.

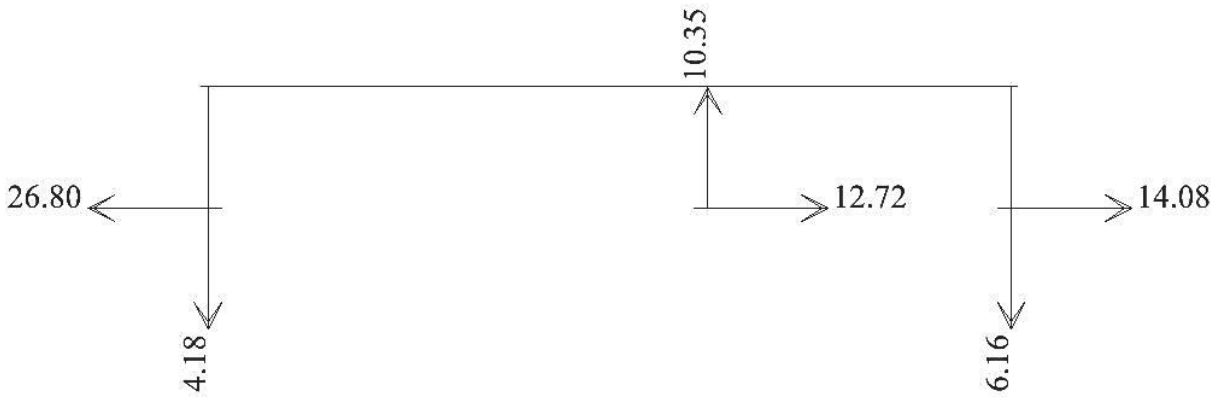

Fig. 4-7 Support Reactions (kips) of Model 2A

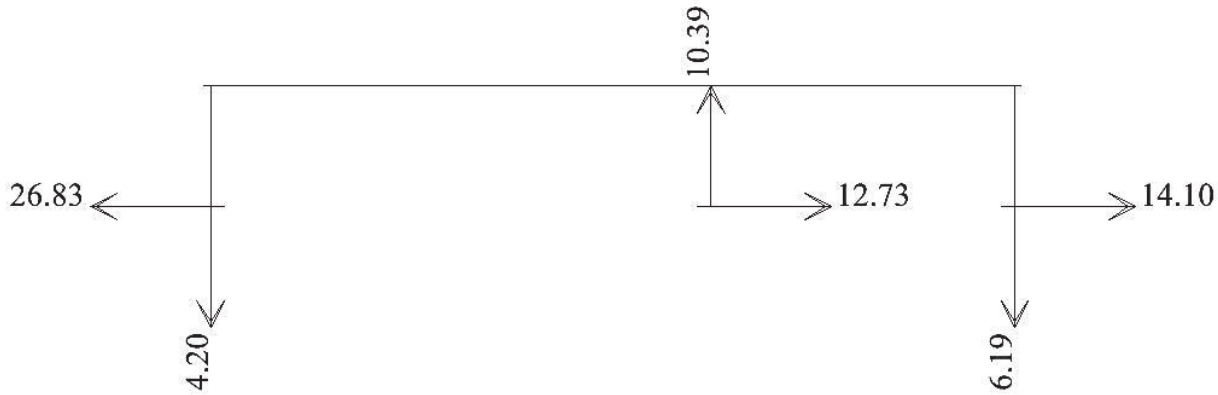

Fig. 4-8 Support Reactions (kips) of Model 2B

The distribution of the axial compressive forces along the post-tensioned continuous concrete beam of Model 2A showed a significant variation with reference to both spans. The left span and the right span had average compressive force of 350.00 kips and 362.64 kips respectively between the centerlines of the exterior columns A and C. These represent average percentage deficits of 6.91% and 3.55% respectively.

Figure 4-9 is the graphical representation of the axial compressive force distribution along both spans of the post-tensioned continuous concrete beam of Model 2A.

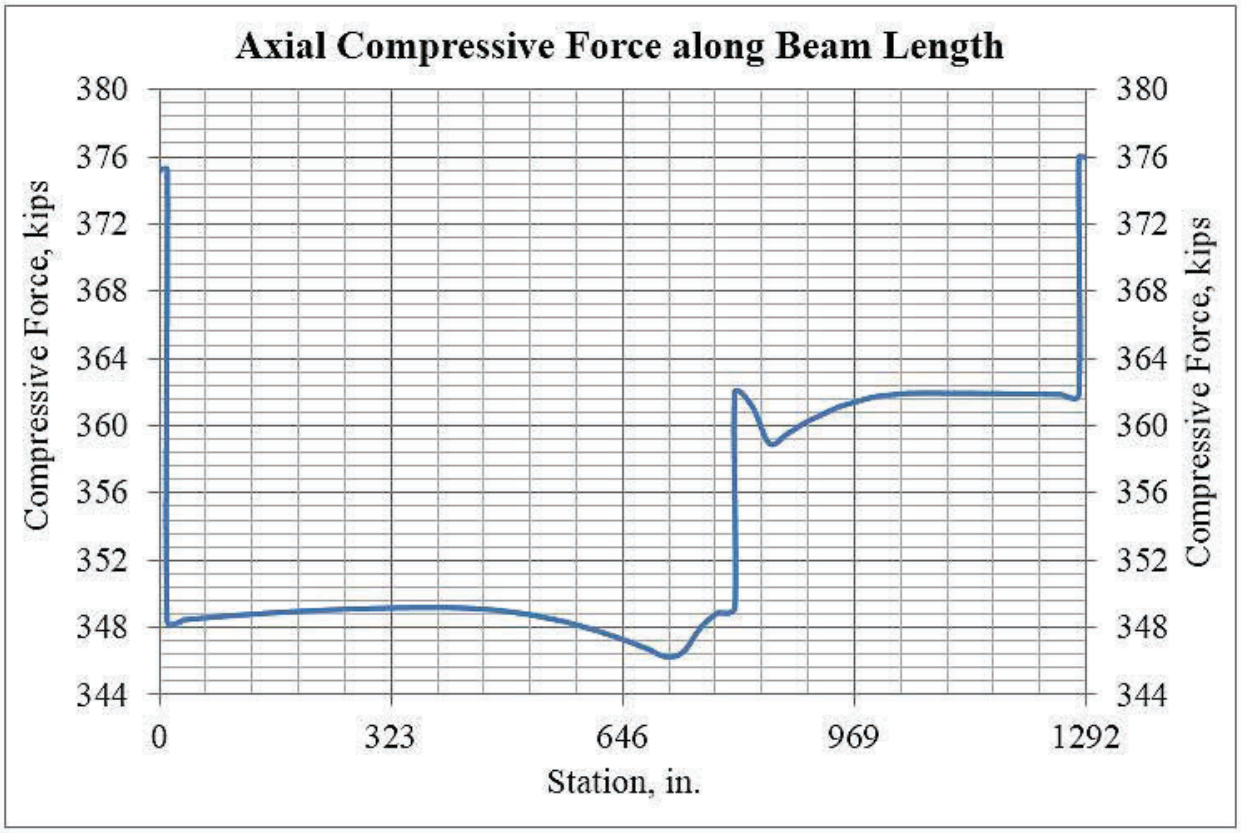

Fig. 4-9 Concrete Beam Compressive Force Distribution of Model 2A

Figure 4-10 shows the stations of interest along the post-tensioned continuous concrete beam where the SAP2000 results of the axial compressive forces of both approaches were taken and tabulated for Model 2.

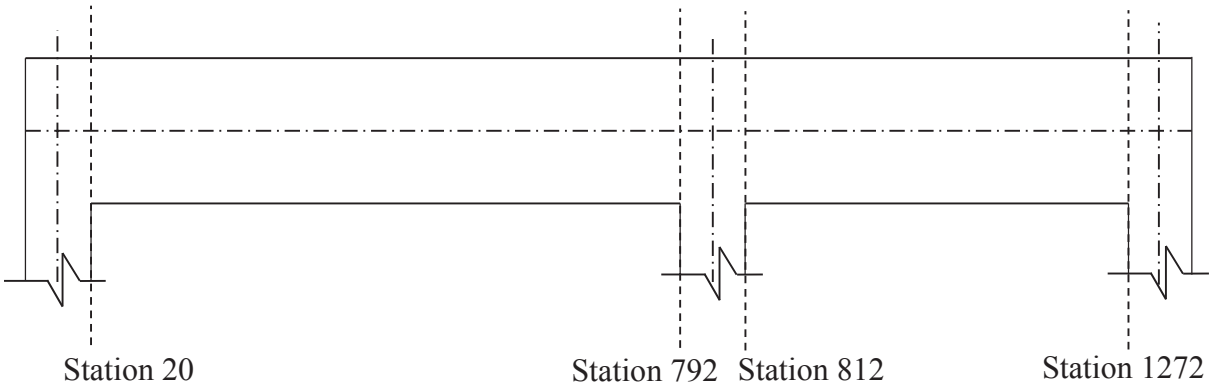

Fig. 4-10 Model 2 Result Stations

Table 4-2 shows the axial compressive forces, absolute discrepancies and their percentage discrepancies at the stations of interest along the post-tensioned continuous concrete beams of Model 2A and Model 2B.

Table 4-2 Axial Compressive Forces along Continuous Beams of Model 2A and Model 2B.

Station, in.	Axial Compressive Force (F), kips		Discrepancy, kips	Discrepancy%
Stations of Interest				
20	Model 2A	-348.422	0.746	0.214
	Model 2B	-349.168		
792	Model 2A	-349.069	0.099	0.028
	Model 2B	-349.168		
812	Model 2A	-361.608	0.295	0.082
	Model 2B	-361.903		
1272	Model 2A	-361.827	0.076	0.021
	Model 2B	-361.903		

Figures 4-11 and 4-12 show the balancing bending moment diagrams (on the tension side) due to initial prestressing force for Model 1A and Model 1B respectively.

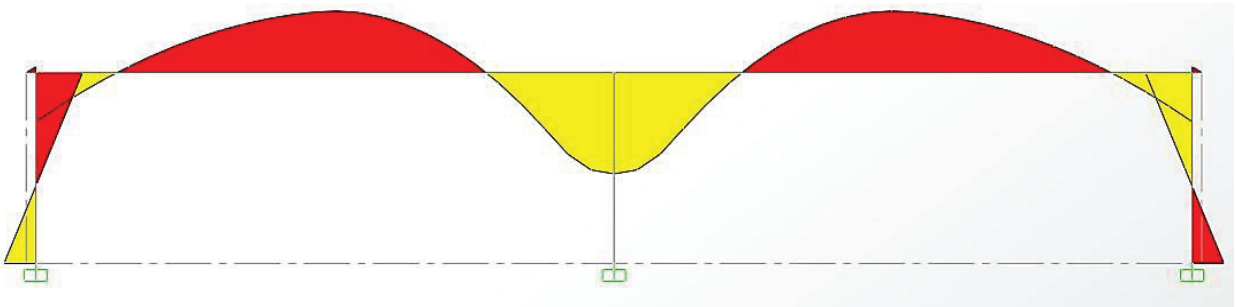

Fig. 4-11 Balancing Bending Moment Diagram (kip-in.) of Model 1A

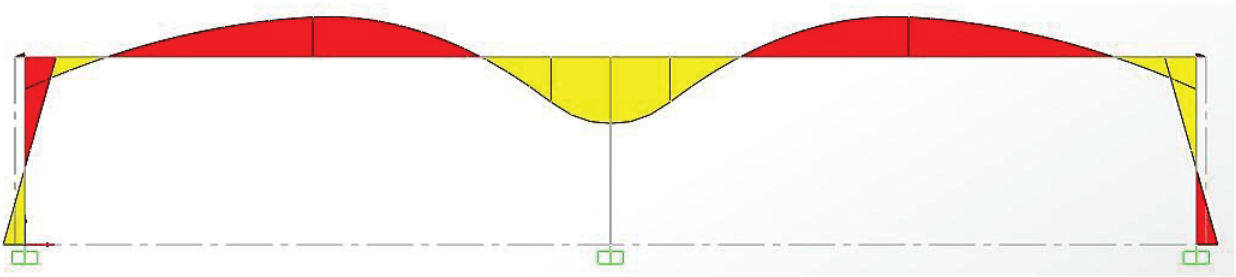

Fig. 4-12 Balancing Bending Moment Diagram (kip-in.) of Model 1B

Figures 4-13 and 4-14 show the balancing bending moment diagrams (on the tension side) due to initial prestressing force for Model 2A and Model 2B respectively.

Fig. 4-13 Balancing Bending Moment Diagram (kip-in.) of Model 2A

Fig. 4-14 Balancing Bending Moment Diagram (kip-in.) of Model 2B

The specified compressive strength of concrete at time of the initial prestress transfer (f'_{ci}) of the post-tensioned continuous concrete beams of Model 1 and Model 2 was computed as follows:

$f'_c = 6{,}000$ psi

$t = 7$ days

$$f'_{ci} = \left(\frac{t}{4 + 0.85t}\right) f_c$$

$$f'_{ci} = \left(\frac{7}{4 + (0.85 \times 7)}\right) \times 6{,}000$$

$$f'_{ci} = 4{,}221.106 \text{ psi} \approx 4{,}221 \text{ psi}$$

Therefore, according to the ACI-318:

Maximum allowable fiber stress in compression $= 0.6f'_{ci}$

$$= 0.6 \times 4221 = 2{,}532.60 \text{ psi}$$

Maximum allowable fiber stress in tension $= 3\sqrt{f'_{ci}}$

$$= 3\sqrt{4221} = 194.91 \text{ psi}$$

Figure 4-15 shows the unbalanced bending moment diagram (on the tension side) due to initial prestressing force for Model 1C.

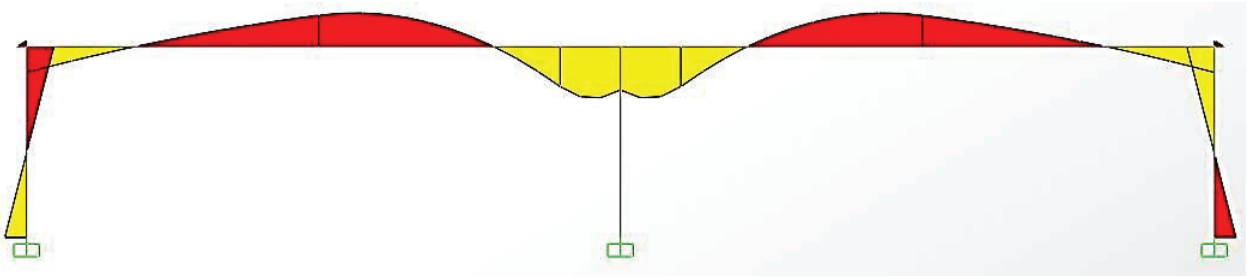

Fig. 4-15 Unbalanced Bending Moment Diagram (kip-in.) of Model 1C

The following is a stepwise computation of the extreme concrete fiber stress due to initial prestressing force at the station of maximum unbalanced bending moment, which is 24" to the left and right of the centerline of the interior column (Stations 586 and 634), along the post-tensioned continuous concrete beam of Model 1C.

Given,

Cross-sectional area, A_c= 600 in^2.

Section modulus relating to the top fibers, S^t = 3,000 in^3.

Section modulus relating to the bottom fibers , S_b= 3,000 in^3.

Compressive force, F = -242,972 Ib (C) < Initial prestressing force, P_i = -260,000 Ib

Moment due to imposed gravity load, M_D = -1,506,460 in.-Ib (Negative moment)

Balancing moment, M_{bi} = 3,161,301 in.-Ib (Positive moment)

Unbalanced moment, M_{ubi} = -1,506,460 + 3,161,301 = 1,654,841 in.-Ib

Top fiber stress, $f^t = -\frac{F}{A_c} - \frac{M_{ubi}}{S^t}$

$f^t = -\frac{242,972}{600} - \frac{1,654,841}{3000}$

f^t = -956.57 psi (C)

Checking the ACI code serviceability requirement:

f^t= 956.57 psi < $0.6f'_{ci}$=2,532.60 psi

Bottom fiber stress, $f_b = -\frac{F}{A_c} + \frac{M_{ubi}}{S_b}$

$f_b = -\frac{242,972}{600} + \frac{1,654,841}{3000}$

f_b=146.66 psi (T)

Checking the ACI code serviceability requirement:

f_b= 146.66 psi < $3\sqrt{f'_{ci}}$=194.91 psi

The procedure outlined for the computation of extreme concrete fiber stresses due to initial prestressing force along the post-tensioned continuous concrete beam of Model 1C is exactly followed for the post-tensioned continuous concrete beam of Model 2C.

Figure 4-16 shows the unbalanced bending moment diagram (on the tension side) due to initial prestressing force of Model 2C.

Fig. 4-16 Unbalanced Bending Moment Diagram (kip-in.) of Model 2C

The cross-sectional area and section modulus of the post-tensioned continuous concrete beam of Model 2 are as follows:

Cross-sectional area, A_c= 640 in^2.

Section modulus relating to the top fibers, S^t = 3,413.33 in^3.

Section modulus relating to the bottom fibers , S_b= 3,413.33 in^3.

The extreme concrete fiber stresses due to initial prestressing before stress losses at the station of maximum unbalanced bending moment, which is 48" to the left of the centerline of the interior column (Station 754), along the post-tensioned continuous concrete beam of Model 2C is illustrated in Table 4-3.

Table 4-3 Extreme Concrete Fiber Stresses along Continuous Beam of Model 2C

Stress Parameter	Model 2C
F, kips	-349.168
M_D, kip-in.	-2,012.343
M_{bi}, kip-in.	4,274.339
M_{ubi}, kip-in.	2,261.996
f^t, psi	-1,208.27 (C) 1,208.27 < 2,532.60
f_b, psi	117.12 (T) 117.12 < 194.91

Hence, for the computation of the concrete fiber stresses for a continuous concrete beam rigidly connected to columns, the horizontal (axial) component of the initial prestressing force is replaced by the concrete axial compressive forces (F). This modification is as a result of restraining effect of the columns taking part of the prestressing force being transferred to the concrete of the beam during post-tensioning.

CHAPTER 5

CONCLUSION

Two two – bay, one – storey concrete frames with post-tensioned continuous concrete beams were modelled and underwent static linear analysis using SAP2000. Two approaches of force application were utilized. The first approach was the application of prestressing through the use of parabolic internal tendons and the second approach was the application of Load Balancing Method (LBM).

This research reinforces the claim that if a prestressed concrete beam is rigidly connected to concrete columns, part of the compressive force in the concrete of the beam is lost to the columns. The losses are translated to the shear reactions at the supports.

Correlation studies between the net axial compressive forces results of both models from both approaches were carried out. The discrepancies were within acceptable limits which depict the accuracy of the balancing loads methodology used. From these concurrence checks, it can be inferred that LBM can be applied to the static frame analysis of post-tensioned concrete beams.

The extreme concrete fiber stresses for both models under LBM were computed. The values obtained were then used to verify their compliance with the ACI-318 serviceability requirement for flexural members.

Lastly, it is common practice to equate the prestressing force to the axial compressive force in computing the axial compressive stress in the concrete beam. However, this research has

proven that the concrete axial compressive force, not the prestressing force, should be used to compute the axial compressive stress of post-tensioned concrete beams in frame analysis.

REFERENCES

Aalami, B. (2000). "Structural Modeling of Post-tensioned Members." *Journal of Structural Engineering*, *ASCE*, Vol. 126, pp. 157-162.

ACI Committee 318 Commentary on Building Code Requirement for Structural Concrete. (2011). American Concrete Institute, Detroit, MI.

Freyermuth, C. (2005). "Segmental Bridges: A Major 21st Century Alternative" Retrieved from http://www.structuremag.org/OldArchives/2005/October%202005/C-CI-Segmental-Concrete-Bridges-Oct-05.pdf

Hurst, M.K. (1998*). Prestress Concrete Design*, 2nd Ed., Wiley, NY.

Kelley, G. (2000). "Prestress Losses in Post-tensioned Structures", *Post-tensioning Concrete Institute Technical Notes*, Phoenix, AR.

Lin, T. (1963). "Load-Balancing Method for Design and Analysis of Prestressed Concrete Structures*." American Concrete Institute*, *Proceedings* Vol. 60, No. 6.

Mohammed, A. W. (2012). "Effects of Axial Component of Prestress in Load Balancing Method". Theses. Paper 802.

Nawy, E.G. (2009). *Prestressed Concrete: A Fundamental Approach*, 5th Ed., Pearson Education, Inc., Upper Saddle River, NJ.

APPENDIX

Table A-1 Sectional Properties of Post-tensioned Continuous Beams for Models 1 and 2

Geometric Properties	Post-tensioned Beam Model 1	Post-tensioned Beam Model 2
Cross-sectional Area, in^2.	600	640
Moment of Inertia (I), in^4.	45000	54613.33
Section Modulus (S), in^3.	3000	3413.33

VITA

Graduate School
Southern Illinois University

Kojo Amponsah Nkuako

kankuako@gmail.com

Institute of Commercial Management, Bournemouth, England
Advanced Diploma, Project Management, November, 2010

Kwame Nkrumah University of Science and Technology, Kumasi, Ghana
Bachelor of Science, Civil Engineering, June 2009

Thesis Title:

Effect of Beam – Column Interaction on Axial Compressive Force in Post–tensioned Continuous Concrete Beam

Major Professor: Dr. J. Kent Hsiao